

Analysis on viewing angle of holographic image reconstructed from digital Fourier hologram in holographic display

Byung Gyu Chae*

Biomedical Imaging Group, Electronics and Telecommunications Research Institute, 218 Gajeong-ro, Yuseong-gu, Daejeon, 34129, South Korea

**bgchae@etri.re.kr*

Abstract: We analyze the viewing angle of holographic image reconstructed from the digital Fourier hologram with an enhanced numerical aperture (NA). The viewing angle of reconstructed image depends on the NA of digital hologram that is determined by a focal length of Fourier lens and hologram size. The enhanced-NA digital hologram reconstructs the image with an angle larger than a diffraction angle of hologram pixel. We also characterize the aliasing effect of digital Fourier hologram, and find that the alias-free region exists even at a high numerical aperture. Numerical simulation and optical experiments are conducted to verify this interpretation of viewing angle of holographic images.

1. Introduction

The digital Fourier hologram reconstructs the holographic image through the Fourier lens in holographic display [1]. The mirror image appears on the opposite side with a focal point symmetry, and thus, the available viewing zone is reduced to a half of object window. Nevertheless, the Fourier holographic system has been utilized to expand the viewing zone by a spatial multiplexing of modulators due to its simple geometry [2-4]. In addition, it has some merit for calculating the digital hologram in comparison to the Fresnel hologram because the specification of object does not change irrespective of the location of an image plane. In the digital Fresnel hologram, the additional operations such as a multi-step Fresnel propagation or scaled Fresnel transform are required to control the image size and pixel interval in accordance with a synthesis distance [5-8].

We have previously studied that the viewing angle of holographic image is determined by means of the hologram numerical aperture (NA) in the Fresnel hologram [9]. That is, the viewing angle is in proportion to the hologram aperture size and inversely proportional to the distance. The digital hologram made at a closer distance shows the viewing angle larger than the diffraction angle by a hologram pixel. We define this type of hologram as the enhanced-NA hologram [10]. In the Fourier hologram, it is expected that the viewing angle of reconstructed image depends on the lens performance to focus the image.

In this study, we analyze the viewing angle of the holographic image reconstructed from the digital Fourier hologram, especially with a high numerical aperture. The aliasing effect occurring in the synthesis of digital hologram with a high numerical aperture is investigated in detail. Numerical simulation is carried

out to observe the change of viewing angle with a reconstructed distance in such a way that computes the propagated diffraction fringe from the image. Finally, we perform the optical experiment to confirm our interpretation for the viewing angle variation.

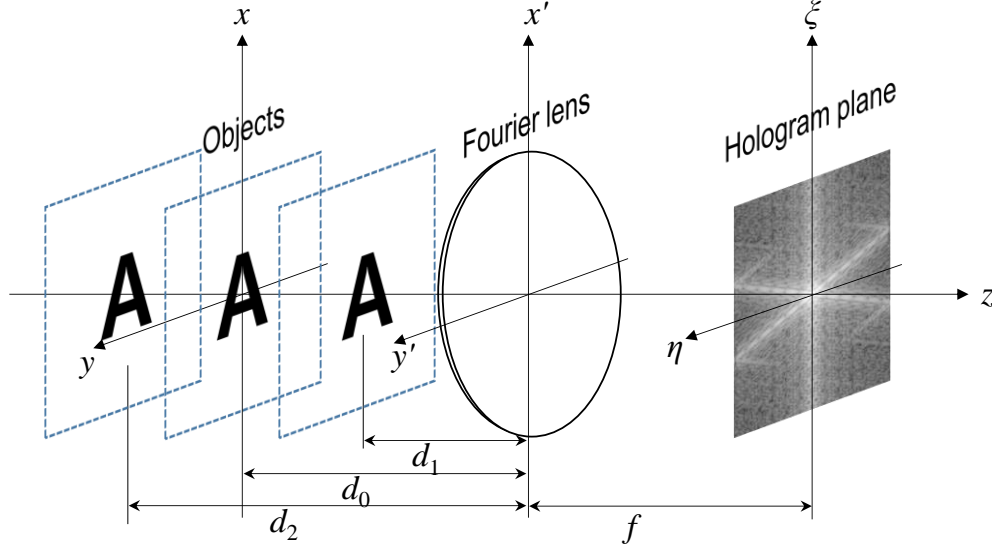


Fig. 1. Schematic diagram for synthesizing the digital Fourier hologram. The letter objects are placed at a distance d in front of the Fourier lens in the direction of propagation of light. The real-valued hologram are drawn in the logarithmic scale.

2. Aliasing effect in digital Fourier hologram

2.1 Analysis on aliasing effect in digital Fourier hologram

The Fourier hologram is calculated from the diffractive wave, $g(\xi, \eta)$ of object through the Fourier lens. The aperture size of lens is assumed to be sufficiently large enough to avoid the vignetting of incident light. As described in Appendix A, the diffraction formula is simply expressed as the Fourier transformation of object field, $O(x, y)$ multiplied by a modified Fresnel factor [1],

$$h_F(\xi, \eta) = \frac{1}{i\lambda f} \exp \left[i \frac{\pi}{\lambda f} \left(1 - \frac{d}{f} \right) (\xi^2 + \eta^2) \right], \quad (1)$$

where the object is located at a distance d in front of the convex lens of focal length f , in Fig. 1:

$$g(\xi, \eta) = \frac{1}{i\lambda f} \exp \left[i \frac{\pi}{\lambda f^2} (\xi^2 + \eta^2) (f - d) \right] \iint O(x, y) \exp \left[-i \frac{2\pi}{\lambda f} (x\xi + y\eta) \right] dx dy. \quad (2)$$

We can obtain the digital hologram by capturing a real or imaginary component of calculated diffraction field. Likewise, the diffraction field itself becomes a complex hologram.

The sampling condition in the object plane is interpreted from the Fourier transform term. Using the frequency component of $\xi/\lambda z$, the relation of pixel resolutions, $\Delta\xi$ of diffractive wave and Δx of the object field is written by

$$\Delta\xi = \frac{\lambda f}{N\Delta x}. \quad (3)$$

For convenience, one-dimensional description for both fields discretized into $N \times N$ pixels is used. The Fourier integral does not include the quadratic phase factor other than the Fresnel transform. When the object field is a slowly varying function, the sampling condition in the object plane is not constrained geometrically because the sampling pitch only has to be chosen to suit the maximum frequency of object field.

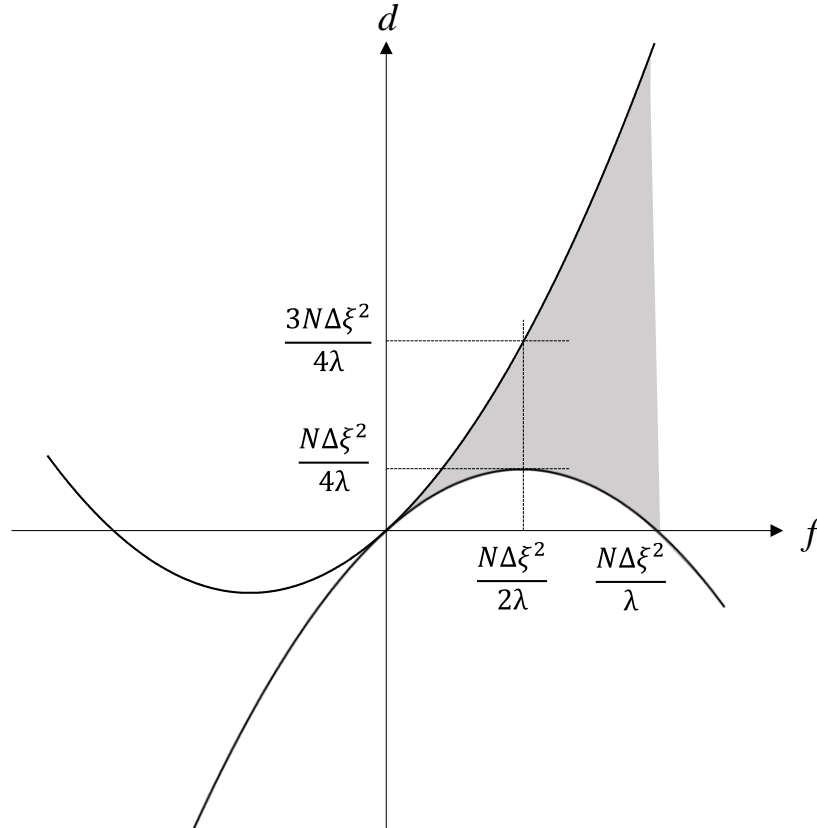


Fig. 2. Graphics to explain alias-free region in the synthesis of digital Fourier hologram. The shadow area between both quadratic functions depicts alias-free region in the enhanced-NA hologram.

On the other hand, although the pixel size of digital hologram is properly defined in Eq. (3), undersampling of diffraction field could take place due to a rapid oscillation of the quadratic phase factor $h_F(\xi, \eta)$ before Fourier transform term. To avoid this type of an aliasing effect in the digital hologram, sampling rate ν_s of diffractive wave should be larger than two times the maximum spatial frequency $\nu_{\xi, \max}$ of the quadratic phase $\phi(\xi, \eta)$, $\nu_s \geq 2\nu_{\xi, \max}$. The maximum frequency $\nu_{\xi, \max}$ is estimated to be

$$\nu_{\xi, \max} = \frac{1}{2\pi} \left| \frac{\partial \phi(\xi, \eta)}{\partial \xi} \right|_{\max} = \left| \frac{\xi_{\max}(f-d)}{\lambda f^2} \right|. \quad (4)$$

The well-sampling condition is given by

$$\Delta \xi^{-1} \geq \left| \frac{N \Delta \xi (f-d)}{\lambda f^2} \right|, \quad (5)$$

where sampling rate is put to be $\Delta \xi^{-1}$, and the relation of hologram field size that $N \Delta \xi = 2|\xi_{\max}|$ is used. To find the constraint of a distance d in the hologram synthesis, one expands above equation as follows,

$$f - \frac{\lambda}{N \Delta \xi^2} f^2 \leq d \leq \frac{\lambda}{N \Delta \xi^2} f^2 + f. \quad (6)$$

As depicted in Fig. 2, the proper region to avoid an aliased error exists between both quadratic functions, which is formed on both sides of the focal plane. Here, a positive value of focal length of lens is considered.

If we define a critical distance z_c as

$$z_c = \frac{N \Delta \xi^2}{\lambda}, \quad (7)$$

the pixel sizes of object and hologram are equal at a critical distance, in Eq. (3). In digital Fresnel hologram, a sampling criterion in the hologram plane is more strict [11-13], where the hologram fringe is undersampled only if the pixel pitch of hologram is larger than that of object field. The digital hologram made at below z_c is classified as the enhanced-NA hologram that invokes the viewing angle of reconstructed image larger than a diffraction angle [10]. Similarly, we define the digital Fourier hologram made by using the Fourier lens with a focal length lower than a critical distance as the enhanced-NA hologram.

We note that there exists the region without an aliased fringe even in the enhanced-NA Fourier hologram. For example, when the focal length in the coordinate of vertex of concave parabola is $z_c/2$, the proper region exists between $z_c/4$ and $3z_c/4$. As the focal length approaches zero, the width of band

decreases, but some proper region remains even at a smaller focal length. We also know that the available region is still valid in the region above the critical distance even though there includes no aliased error initially.

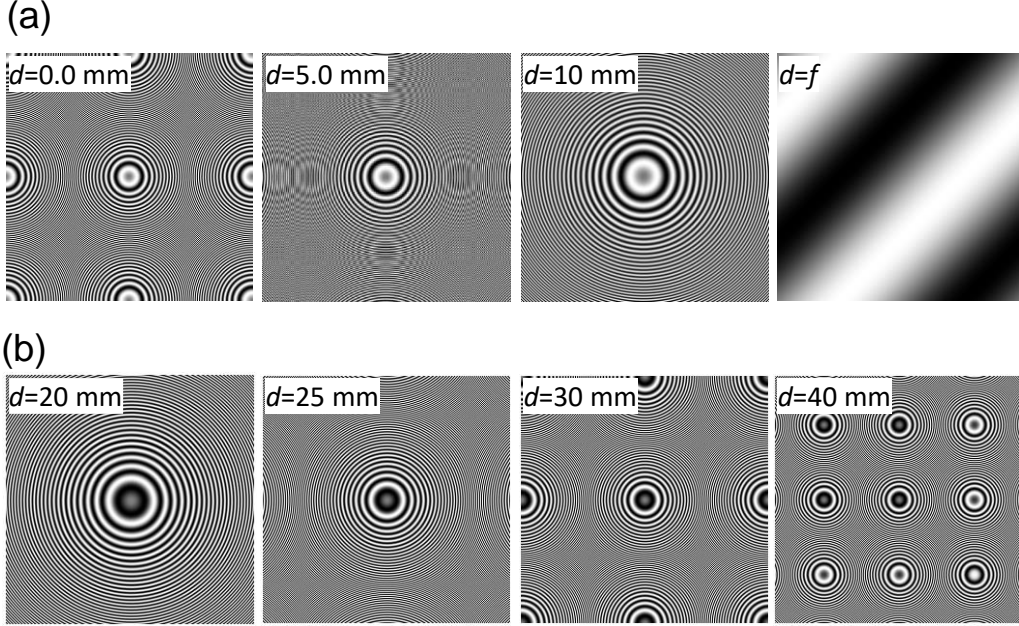


Fig. 3. Digital Fourier hologram synthesized by using point object located at various distances (a) in front of focal plane and (b) behind focal plane. The specifications are as follows; wavelength $\lambda = 532$ nm, focal length $f = 15.4$ mm, pixel number $N = 256$, and pixel pitch $\Delta\xi = 8$ μm .

Figure 3 shows the digital Fourier hologram made by using a point object located at various distances. The on-axis hologram is made using the coaxial plane wave as a reference wave. The digital hologram has 256×256 pixels with a pixel pitch of $8 \mu\text{m}$. Using an incident plane wave of wavelength 532 nm, the critical distance z_c is 30.8 mm. The focal length is set to be 15.4 mm, which is the value of $z_c/2$ at the vertex in Fig. 2. In this circumstance, the object has a pixel size of $4 \mu\text{m}$.

When the depth value of d is equal to be zero, the quadratic phase term coincides with the Fresnel factor in the Fresnel diffraction. The hologram of point object is represented as Fresnel zone [14], where the alias-free region can exist above the critical distance, as depicted in Fig. 2. Figure 3(a) illustrates the four aliased fringes in two-dimensional space generated from the undersampling of Fresnel factor. As the object plane approaches the focal plane, the aliased fringes disappear. When the distance d is larger than a quarter of z_c , 7.7 mm, there appears no replica zones. We find that the phase coefficient described by a finite depth d alleviates the aliasing effect of fringe. In the focal plane, this type of aliased error does not occur. Here, if the point object places at an exact center, the hologram would have the uniformly distributed intensity. As

the distance d increases beyond a focal length, replica fringes are regenerated. The proper region showing no aliased fringes exists between $z_c/4$ and $3z_c/4$, which is well consistent with the graphical interpretation of Fig. 2. We also confirmed that this phenomenon is applied for other focal lengths.

2.2 Aliasing effect in digital Fourier hologram synthesized by using extended field of view of object

The object field size in the hologram synthesis is confined on the basis of the relation of Eq. (3). When the focal length of Fourier lens is a half of z_c , the object has a pixel pitch of $4\text{ }\mu\text{m}$, and thus, the object size is a half of hologram size. We investigate the aliasing effects of hologram fringe when the hologram is generated by using the extended object field outside the diffraction area by a hologram pixel. We consider the object field with 512×512 pixels so that its physical size of $2048 \times 2048\text{ }\mu\text{m}^2$ matches with that of digital hologram. Figure 4 illustrates the digital hologram by using an off-axis point object placed at (32,256) pixel position. Putting (256,256) pixel point as the origin, this off-axis point object is located outside the diffraction area. The Fresnel zones places at a shifted position. The lateral location of off-axis point object induces a phase shifting factor from the Fourier transform of delta function. We see that although the depth increases, the replica fringes in the center does not disappear completely.

In the digital hologram made by using a point object placed at (1,256) position, the hologram fringe pattern changes as like that of digital hologram in Fig. 3(a). Since the point object is located at the center of extended area, the phase shifting factor from the Fourier transform repeats one period where the repeated fringe is exactly generated at the center. We have observed that in the digital Fresnel hologram, the replica fringes are suppressed due to a concentration of diffractive wave from the real object with a finite size in the Fresnel regime [10]. However, this phenomenon is difficult to arise in the digital Fourier hologram because the diffractive wave is spread out at a close distance to focal plane.

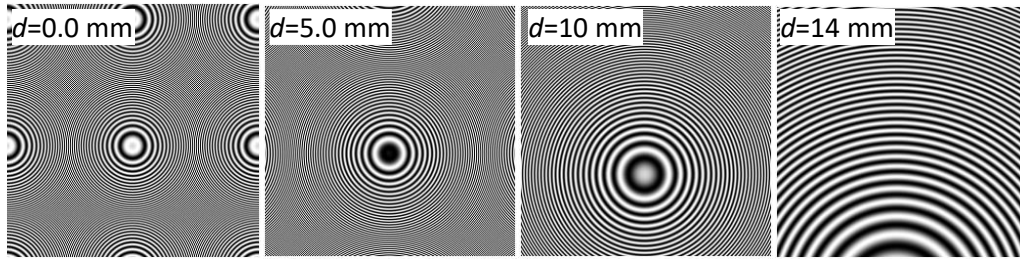


Fig. 4. Digital Fourier hologram synthesized by using a point object placed at the extended area. The focal length of lens and pixel size of hologram are kept to be 15.4 mm and $8\text{ }\mu\text{m}$, respectively.

3. Analysis of viewing angle of reconstructed image from digital Fourier hologram

Figure 5 shows the schematic diagram for the reconstructed images through the Fourier lens using digital Fourier hologram. As described in Appendix B, the diffractive field through this system is expressed as the inverse diffraction of Eq. (2):

$$O(x, y) = \frac{1}{i\lambda f} \iint g(\xi, \eta) \exp \left[-i \frac{\pi}{\lambda f^2} (\xi^2 + \eta^2) (f - d) \right] \exp \left[i \frac{2\pi}{\lambda f} (x\xi + y\eta) \right] d\xi d\eta. \quad (8)$$

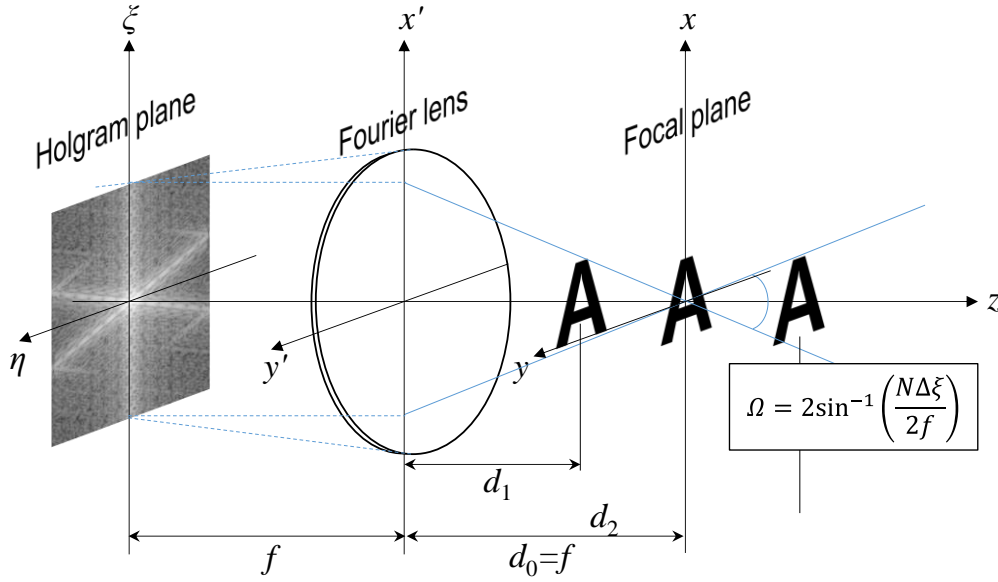


Fig. 5. Schematic diagram of the Fourier holographic display. The letter images are formed at a distance behind the Fourier lens. The real-valued holograms are drawn in the logarithmic scale.

We consider the sampled Fourier hologram $g_s(\xi, \eta)$, which is loaded on the pixelated modulator with pixel interval p and width Δp in the (ξ, η) coordinates:

$$g_s(\xi, \eta) = \sum_{n_\xi=-\infty}^{\infty} \sum_{n_\eta=-\infty}^{\infty} \left[g(n_\xi p_\xi, n_\eta p_\eta) \text{rect} \left(\frac{\xi - n_\xi p_\xi}{\Delta p_\xi}, \frac{\eta - n_\eta p_\eta}{\Delta p_\eta} \right) \right], \quad (9)$$

where $\text{rect}()$ is a rectangular function. After some operation, we obtain the diffractive object wave propagating from the hologram as follows [9],

$$O(x, y) = C \sum_{\alpha=-\infty}^{\infty} \sum_{\beta=-\infty}^{\infty} \iint g(\xi, \eta) \exp [ik(\xi \sin \theta_\alpha + \eta \sin \theta_\beta)] \exp \left[-i \frac{2\pi}{\lambda} \left(\frac{\Delta z(\xi^2 + \eta^2)}{2f^2} - \frac{x\xi + y\eta}{f} \right) \right] d\xi d\eta. \quad (10)$$

The high-order diffraction beams propagate at an angle θ . Here, C includes the modulation of sinc function due to a hologram pixel pitch, and $\Delta z = f - d$. As described in the sampled Fresnel hologram [9], the pixelated structure induces only high-order diffraction images. The specification of hologram synthesis depends on the sampling rate, but each diffraction formula in summation sign could be interpreted as a wave propagation separately.

From this interpretation, we can extract that the viewing angle is not restricted to the diffraction angle. Considering the hologram with a finite aperture size L , $g(\xi, \eta) \text{rect}(\xi/L, \eta/L)$, each diffraction formula is expanded as a convolutional form as follows,

$$O(x, y) = \frac{1}{i\lambda f} \mathbf{FT} \{ g(\xi, \eta) h_F(x, y) \} * \mathbf{FT} \left\{ \text{rect} \left(\frac{\xi}{L}, \frac{\eta}{L} \right) \right\}. \quad (11)$$

The asterisk denotes a convolution operation. In the hologram function of a point object, the first term of Fourier transform \mathbf{FT} becomes delta function, because the complex hologram of a point object is equal to the modified Fresnel factor of Eq. (1). The object image is calculated to be in the form of a sinc function:

$$O(x, y) = \left(\frac{L}{\lambda f} \right)^2 \text{sinc} \left(\frac{\pi x L}{\lambda f} \right) \text{sinc} \left(\frac{\pi y L}{\lambda f} \right). \quad (12)$$

The width of the first maximum peak of a sinc function indicates a measure resolving the closest points. The real object with a finite extent can be regarded as a collection of individual point objects. Therefore, the resolution limits $R_{x,y}$ of object would be

$$R_x = \frac{\lambda f}{N_\xi \Delta \xi} \quad \text{and} \quad R_y = \frac{\lambda f}{N_\eta \Delta \eta}. \quad (13)$$

These values are explained on the basis of the Abbe criterion by the hologram numerical aperture [15,16], $\text{NA} = \sin \Omega_{\text{NA}} = (N_\xi \Delta \xi) / (2f)$. As illustrated in Fig. 5, since the converging and diverging waves have a mirror symmetry with respect to a focal plane, the viewing angle Ω of a reconstructed image can be written in the form:

$$\Omega = 2 \sin^{-1} \left(\frac{N_\xi \Delta \xi}{2f} \right). \quad (14)$$

We note that in the Fourier hologram, the viewing angle of reconstructed images depends on only the aperture extent of digital hologram and focal length of Fourier lens, which is irrespective of the imaging plane of object. Fundamentally, the ability to focus the light is defined by the lens performance, and thus, the resolution of reconstructed images at a different distance d would be the same. This interpretation is not limited to the enhanced-NA hologram, and would be applied to general digital Fourier hologram.

On the other hand, the whole area of digital hologram, other than the lateral extent of diffraction wave passing through the Fourier lens, plays a role in aperture. The diffracted wave from the hologram would occupy the lateral space larger than the hologram size. Therefore, the NA of lens increases, but it is interesting that the resolution of reconstructed image is confined by the hologram numerical aperture. When the image is formed near the back focal plane, the location of hologram plane is not restricted to the focal plane. As referred to Appendix A, this configuration contributes to only the phase factor before the Fourier transform term, and thus, it does not affect the measured intensity of image, where the viewing angle of image does not change. These properties will be proved by means of numerical simulation and optical experiments.

4. Numerical analysis of viewing angle of reconstructed image from digital Fourier hologram

Figure 6 illustrates the numerical studies for observing the viewing angle of reconstructed image from the digital Fourier hologram. Three kinds of digital holograms are prepared by using the ‘HOLO’ letter objects placed at d_0 , d_1 , and d_2 distances in Fig. 1. The hologram has 256×256 size with a pixel pitch of $8 \mu\text{m}$. The coherent plane wave of 532-nm wavelength and the Fourier lens with a focal length of 30.8 mm are used.

To investigate an angular field of view of the reconstructed holographic image, the diffraction fringes far away from the imaging plane are numerically calculated via the reverse diffraction formula of Eq. (8). The diffraction fringes are calculated as a function of distance d , where the diffraction fringe is an intensity pattern of the diffracted wave. We observed that in the real-valued or imaginary-valued hologram, the conjugated image is formed on the opposite plane with respect to the focal plane. In order to measure the change in the diffraction fringe clearly, we used a complex amplitude hologram without showing the overlap of a conjugate image.

The diffraction fringes are displayed with a logarithmic scale to mitigate the energy concentration at the origin in the Fourier space. The total field size does not change with a distance d due to a constant focal length. Based on Eq. (3), the pixel pitch of object is $8 \mu\text{m}$, and thus, the sizes of both object and hologram are the same as $2048 \times 2048 \mu\text{m}^2$. As shown in Fig. 6, we can observe the apparent diffraction fringe corresponding to the letter image propagation, while it is not clearly distinguishable in a linear-scale image. This active area in an inset box increases with increasing a distance.

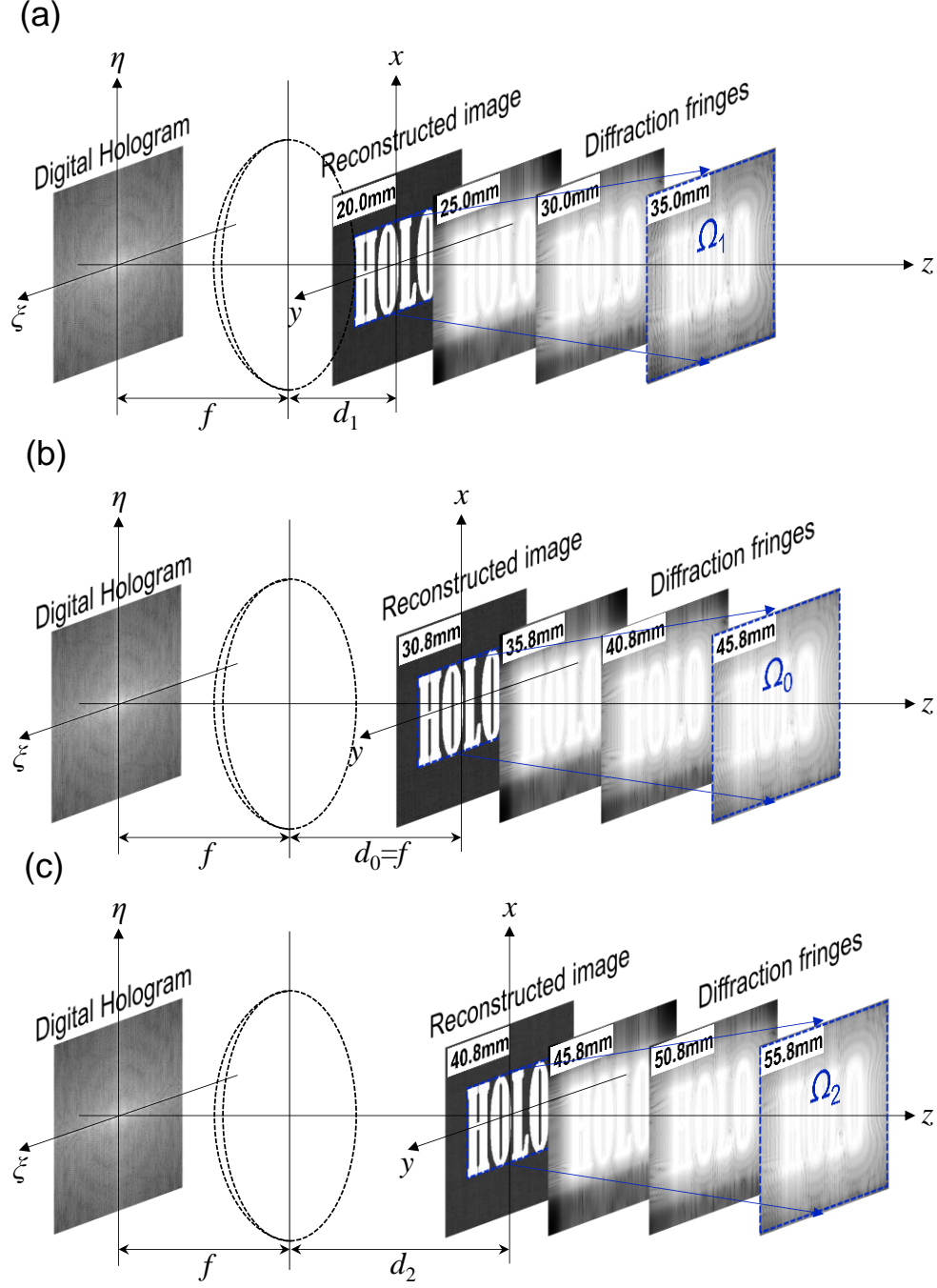


Fig. 6. Numerical studies for observing the viewing angle of reconstructed image from the digital Fourier hologram. The diffraction fringe propagated from the imaging plane located at distances of (a) $d_1 = 20.0$ mm, (b) $d_0 = 30.8$ mm, and (c) $d_2 = 40.8$ mm. All images together with digital hologram are drawn in the logarithmic scale.

The diffraction behavior from the hologram made at a d_1 -distance is displayed in Fig. 6(a). The image is formed at a d_1 -distance before the focal plane. The active diffraction area in the blue box changes from

960 μm at 20-mm distance of d in the image plane to 1648 μm at 30-mm distance. The viewing angle Ω_1 of 3.94° is estimated from a growth rate of the diffraction fringe along a distance. This value is similar to the diffraction angle due to the pixel pitch. Figure 6(b) depicts the diffraction behavior of a reconstructed image for the hologram made at d_0 -distance, where the image is formed at the focal plane. The viewing angle Ω_0 estimated from the increase of the active diffraction fringe is about 3.85° . Figure 6(c) is the diffraction result for the hologram made at d_2 -distance. The image is reconstructed at d_2 -distance behind the focal plane. The active diffraction area increases similarly with previous results, where the angle Ω_2 is estimated to be 3.8° .

We find that the viewing angle of reconstructed image from the Fourier hologram does not depend on the depth quantity of d , which is irrespective of a location of imaging plane. These values are consistent with the theoretical quantity of 3.81° in Eq. (14). Only the lens performance to focus the light determines the viewing angle of reconstructed image. We also find that the appropriate aperture extent is defined by the whole area of digital hologram because the lateral size of diffractive wave in the lens plane is two times the hologram size.

Figure 7 is the simulation results for the enhanced-NA hologram synthesized through the Fourier lens with a focal length of $z_c/2$. To compare their viewing angle variations clearly, all the objects are enlarged with 512×512 size using the zero-padding. The small ratio of active area enables us to investigate the change of viewing angle apparently. In this case, the critical distance z_c appears to be 61.6 mm. We used the Fourier lens with focal length of a half of z_c , 30.8 mm, where the object pixel size is 4 μm and thus, the reconstructed image size is a half of the hologram size. We note that the active diffraction region reveals a rapid increase. The active area increases from 480 μm at 30.8-mm distance to 1368 μm at 37.8-mm distance. The viewing angle Ω is calculated to be approximately 7.25° , whose value is approximately twice the diffraction angle of 8- μm pixel.

This result shows that the viewing angle of a reconstructed image is simply determined by the numerical aperture of digital hologram. The angle value reaches 27.5° at a 7.7-mm distance.

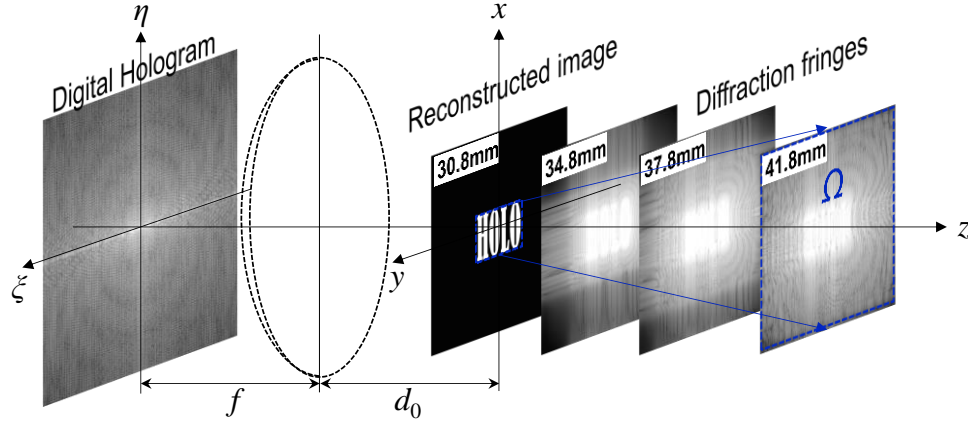


Fig. 7. The diffraction fringe reconstructed from the digital hologram made by using the Fourier lens with a focal length of a half of critical distance. The enhanced viewing angle of reconstructed image appears.

5. Optical hologram imaging for digital Fourier hologram and its discussion

We generated digital hologram by using two letter objects separated from each other in the axial direction, in Fig. 8(a). Since the Fourier hologram reconstructs twin image formed with a focal point symmetry, a half of object window is utilized to avoid a direct beam and an overlap of the images. Two objects are vertically stacked on the coaxial x -axis in order to observe their parallax conveniently. This configuration is very useful to measure a smaller viewing angle. We used a phase spatial light modulator (Holoeye Photonics AG) with 1920×1200 pixels and a pixel pitch of $8.1 \mu\text{m}$. The blue laser with a 473-nm wavelength was utilized as the source of incident plane wave. The random phase is added to the object to diffuse the concentration of hologram fringe [17,18].

Figure 8(b) shows the image reconstructed from the hologram made using the Fourier lens with a focal length of 250 mm, whose value is close to the z_c -distance of 266.3 mm for x -direction. The former letter is located at a distance of 230 mm from the Fourier lens, and the separation of two objects is put to be 20 mm. The hologram plane is placed on the front focal plane of Fourier lens, as illustrated in Fig. 5, but we confirmed that the image is well reconstructed even though the hologram is not located on the focal plane. As described in Section 2, the phase factor generated from this configuration would not affect the image intensity.

The captured image shows apparently an accommodation effect where the first image is focused. The image is acquired through a spatial filtering blocking the direct beam and high-order images. When one changes the viewing direction, the latter image would be placed at a horizontally shifted position owing to a different perspective view. The picture below of Fig. 8(b) is the image captured at a maximally changed

viewing direction, where the latter image is slightly shifted. The estimated quantity of viewing angle is about to be 3.0° , which is close to the calculated value of 3.56° . In the z_c -distance, since the diffraction angle by a hologram pixel is equal to the viewing angle of restored image, this quantity is similar to the diffraction angle.

Figure 8(c) is the restored image from the hologram made using the Fourier lens with a focal length of 150 mm. The former letter is focused at a distance of 130 mm and the separation of two objects is still 20 mm. We can see that the latter image is largely shifted in comparison to that of Fig. 8(a), which indicates that the viewing angle increases. The viewing angle is estimated to be 5.7° from the maximum perspective view of the reconstructed image, which is close to the calculated value of 5.94° . Here, we observe that the high-order images also show the shifted latter image. The images adjacent to the central image show their perspective views in this viewing direction. Twin image showing on the opposite plane with a respect to focal plane is displayed in Fig. 8(d). The image shape is inverted, and the estimated viewing angle has a similar value.

As not displayed here, we also confirmed that the viewing angle of reconstructed image from the digital hologram made by using the object placed at a different distance d does not change. We know that the digital hologram made at a distance lower than the value in well-sampling condition forms the replica fringes, as explained in Section 2. In this situation, discreet approaches may be sensible in defining the hologram aperture size. The quantum mechanical approaches in our previous work showed that whole area of hologram becomes the numerical aperture size for individual replica fringes [19].

We studied that in the Fresnel hologram, the viewing angle of reconstructed image at a closer distance is larger [9]. In this case, there includes no lens to generate the image in compliance with the lens formula. The hologram itself makes the focused image, where the ability to collect a light would depend on the imaging plane. The NA of digital Fresnel hologram changes in accordance with a reconstructed distance. However, the viewing angle in the digital Fourier hologram does not depend on the location of the imaging plane with being a constant focal length of Fourier lens. The viewing angle of optically restored images well complies with Eq. (14). Here, we find that the extent of diffractive wave in the lens plane is twice the hologram size, but the aperture size is defined by the hologram size. The Fourier hologram has a constant NA determined by the aperture extent of hologram and focal length of lens.

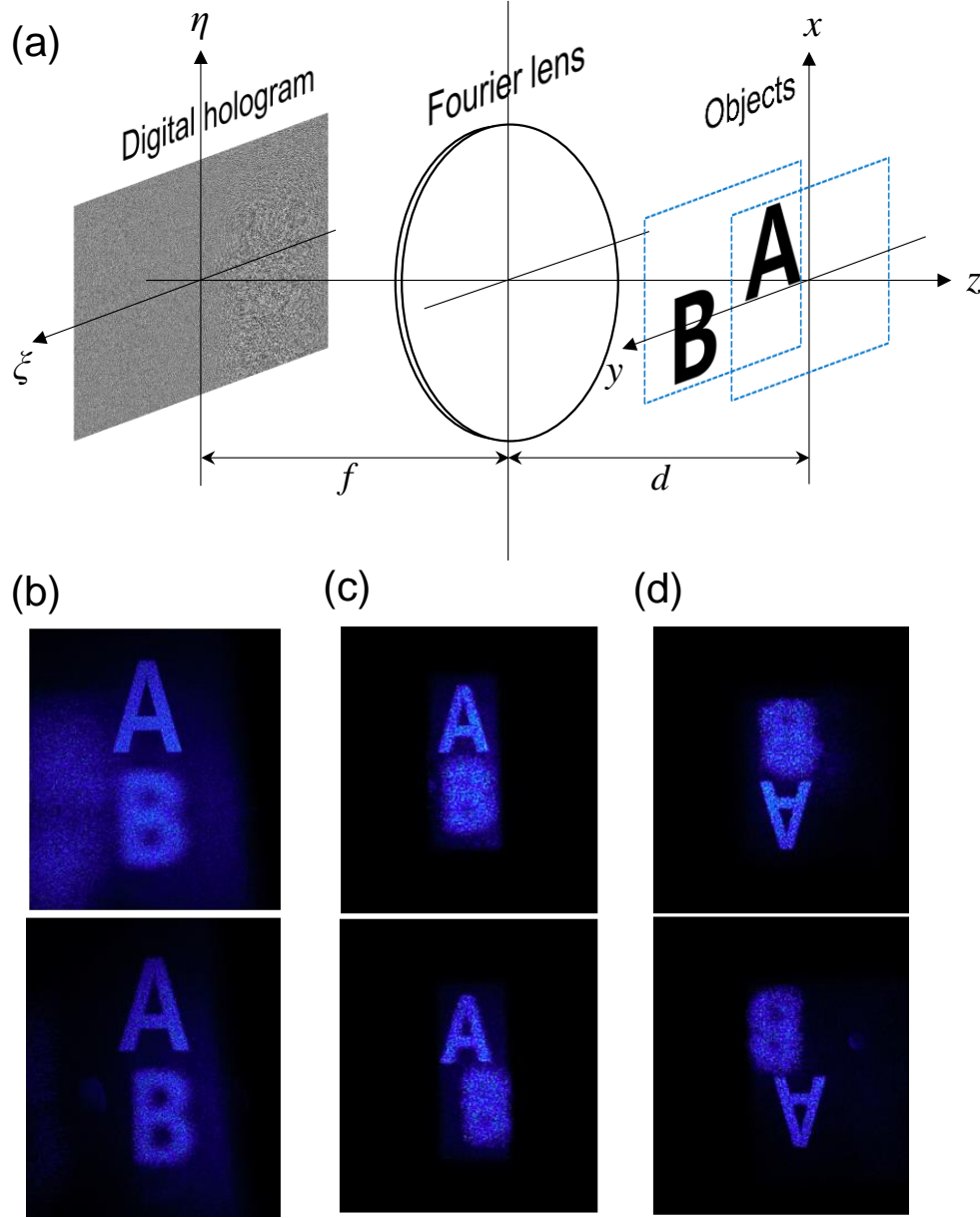


Fig. 8. Optical experiments for reconstructing the image from the digital Fourier hologram. (a) Configuration of the hologram synthesis using two separated letter objects. (b) Reconstructed images from the digital hologram made by using the Fourier lens with a focal length of 250 mm. (c) Original images and (d) twin images reconstructed from the digital hologram made by using the Fourier lens with a focal length of 150 mm. All of pictures below are the captured images in the maximally shifted viewing direction.

6. Conclusions

The aliasing effect of digital Fourier hologram is investigated, where the alias-free region exists even in the digital hologram with a high numerical aperture. The numerical aperture is determined by the lens

performance to focus the image. The viewing angle of reconstructed image depends on the numerical aperture of digital hologram, whose property is not restricted to the enhanced-NA Fourier hologram. We observe in the numerical simulation that the viewing angle of restored image increases with decreasing a focal length irrespective of the location of an image plane. Optical experiments show the consistent result with this analysis of viewing angle of reconstructed holographic images.

Appendix A: Field distribution of forward propagation through the Fourier lens

Field distribution $g(\xi, \eta)$ propagating through the optical system can be expressed as the linear integral form due to a linearity of wave propagation,

$$g(\xi, \eta) = \iint h(\xi, \eta; x, y) O(x, y) dx dy. \quad (\text{A1})$$

The optical system is completely interpreted when the impulse response function $h(\xi, \eta; x, y)$ with respect to object field $O(x, y)$ is found. In Fig. 1, the complex field $g_d(x', y')$ in the plane placed against the lens is written by the Fresnel propagation:

$$g_d(x', y') = \iint O(x, y) \exp\left\{i \frac{\pi}{\lambda d} [(x - x')^2 + (y - y')^2]\right\} dx dy, \quad (\text{A2})$$

where constant phase factor is dropped, and d is a propagation distance. The field distribution $g_l(x', y')$ immediately after lens of a focal length f is given by

$$g_l(x', y') = g_d(x', y') \exp\left[-i \frac{\pi}{\lambda f} (x'^2 + y'^2)\right]. \quad (\text{A3})$$

We obtain the field distribution in the back focal plane of the Fourier lens as like,

$$g(\xi, \eta) = \iint g_l(x', y') \exp\left\{i \frac{\pi}{\lambda f} [(x' - \xi)^2 + (y' - \eta)^2]\right\} dx' dy'. \quad (\text{A4})$$

The impulse function becomes the integral form at lens coordinates (x', y') , which can be calculated by using the Gaussian integral formula:

$$\begin{aligned} h(\xi, \eta; x, y) &= \exp\left[i \frac{\pi}{\lambda f} (\xi^2 + \eta^2)\right] \exp\left[i \frac{\pi}{\lambda d} (x^2 + y^2)\right] \\ &\times \iint \exp\left[i \frac{\pi}{\lambda d} (x'^2 + y'^2)\right] \exp\left\{-i \frac{2\pi}{\lambda} \left[x' \left(\frac{x}{d} + \frac{\xi}{f}\right) + y' \left(\frac{y}{d} + \frac{\eta}{f}\right)\right]\right\} dx' dy' \\ &= \frac{1}{i\lambda f} \exp\left[i \frac{\pi}{\lambda f^2} (\xi^2 + \eta^2) (f - d)\right] \exp\left[-i \frac{2\pi}{\lambda f} (x\xi + y\eta)\right]. \end{aligned} \quad (\text{A5})$$

We can get the final form of complex field [1]:

$$g(\xi, \eta) = \frac{1}{i\lambda f} \exp \left[i \frac{\pi}{\lambda f^2} (\xi^2 + \eta^2) (f - d) \right] \iint O(x, y) \exp \left[-i \frac{2\pi}{\lambda f} (x\xi + y\eta) \right] dx dy. \quad (\text{A6})$$

Appendix B: Field distribution of inverse propagation through the Fourier lens

The complex field $g_f(x', y')$ inversely propagated from the hologram $g(\xi, \eta)$ to the plane placed against the lens is expressed as the Fresnel propagation, in Fig. 4:

$$g_f(x', y') = \iint g(\xi, \eta) \exp \left\{ -i \frac{\pi}{\lambda f} \left[(x' - \xi)^2 + (y' - \eta)^2 \right] \right\} d\xi d\eta. \quad (\text{B1})$$

The field distribution $g_l(x', y')$ immediately after lens is written by

$$g_l(x', y') = g_f(x', y') \exp \left[i \frac{\pi}{\lambda f} (x'^2 + y'^2) \right]. \quad (\text{B2})$$

We obtain the field distribution in the back focal plane of the Fourier lens as like,

$$O(x, y) = \iint g_l(x', y') \exp \left\{ -i \frac{\pi}{\lambda d} \left[(x - x')^2 + (y - y')^2 \right] \right\} dx' dy'. \quad (\text{B3})$$

The impulse function $h(x, y; \xi, \eta)$ is given by

$$O(x, y) = \iint h(x, y; \xi, \eta) g(\xi, \eta) d\xi d\eta. \quad (\text{B4})$$

The impulse function becomes the integral form at the lens coordinates (x', y') and is calculated to be as follows,

$$\begin{aligned} h(x, y; \xi, \eta) &= \exp \left[-i \frac{\pi}{\lambda f} (\xi^2 + \eta^2) \right] \exp \left[-i \frac{\pi}{\lambda d} (x^2 + y^2) \right] \\ &\quad \times \iint \exp \left[-i \frac{\pi}{\lambda d} (x'^2 + y'^2) \right] \exp \left\{ i \frac{2\pi}{\lambda} \left[x' \left(\frac{x}{d} + \frac{\xi}{f} \right) + y' \left(\frac{y}{d} + \frac{\eta}{f} \right) \right] \right\} dx' dy' \\ &= \frac{1}{i\lambda f} \exp \left[-i \frac{\pi}{\lambda f^2} (\xi^2 + \eta^2) (f - d) \right] \exp \left[i \frac{2\pi}{\lambda f} (x\xi + y\eta) \right]. \end{aligned} \quad (\text{B5})$$

We obtain the final form of inverse propagation:

$$O(x, y) = \frac{1}{i\lambda f} \iint g(\xi, \eta) \exp \left[-i \frac{\pi}{\lambda f^2} (\xi^2 + \eta^2) (f - d) \right] \exp \left[i \frac{2\pi}{\lambda f} (x\xi + y\eta) \right] d\xi d\eta. \quad (\text{B6})$$

Funding

This work was partially supported by Institute for Information & Communications Technology Promotion (IITP) grant funded by the Korea government (MSIP) (2017-0-00049).

Disclosures

The author declares no conflicts of interest.

References

1. J. W. Goodman, Introduction to Fourier Optics (McGraw-Hill, 1996).
2. N. Fukaya, K. Maeno, O. Nishikawa, K. Matsumoto, K. Sato, and T. Honda, "Expansion of the image size and viewing zone in holographic display using liquid crystal devices," Proc. SPIE **2406**, 283-289 (1995).
3. K. Yamamoto, Y. Ichihashi, T. Senoh, R. Oi, and T. Kurita, "3D objects enlargement technique using an optical system and multiple SLMs for electronic holography," Opt. Express **20**(19), 21137-21144 (2012).
4. J. Hahn, H. Kim, Y. Lim, G. Park, and B. Lee, "Wide viewing angle dynamic holographic stereogram with a curved array of spatial light modulators," Opt. Express **16**(16), 12372-12386 (2008).
5. F. Zhang, I. Yamaguchi, and L. P. Yaroslavsky, "Algorithm for reconstruction of digital holograms with adjustable magnification," Opt. Lett. **29**(14), 1668-1670 (2004).
6. D. G. Voelz and M. C. Roggemann, "Digital simulation of scalar optical diffraction: revisiting chirp function sampling criteria and consequences," Appl. Opt. **48**(32), 6132-6142 (2009).
7. T. Shimobaba, T. Kakue, N. Okada, M. Oikawa, Y. Yamaguchi, and T. Ito, "Aliasing-reduced Fresnel diffraction with scale and shift operations," J. Opt. **15**, 075405 (2013).
8. J.-P. Liu, "Controlling the aliasing by zero-padding in the digital calculation of the scalar diffraction," J. Opt. Soc. Am. A **29**(9), 1956-1964 (2012).
9. B. G. Chae, "Analysis on angular field of view of holographic image dependent on hologram numerical aperture in holographic display," Opt. Eng. **59**(3), 035103 (2020).
10. B. G. Chae, "Analysis on image recovery for on-axis digital Fresnel hologram with aliased fringe generated from self-similarity of point spread function," Opt. Commun. **466**, 125609 (2020).
11. D. Mas, J. Garcia, C. Ferreira, L. M. Bernardo, and F. Marinho, "Fast algorithms for free-space diffraction patterns calculations," Opt. Commun. **164**, 233-245 (1999).

12. A. Stern and B. Javidi, "Improved-resolution digital holography using the generalized sampling theorem for locally band-limited fields," *J. Opt. Soc. Am. A* **23**(5), 1227-1235 (2006).
13. L. Onural, "Some mathematical properties of the uniformly sampled quadratic phase function and associated issues in Fresnel diffraction simulations," *Opt. Eng.* **43**(11), 2557-2563 (2004).
14. T. C. Poon and J. P. Liu, *Introduction to Modern Digital Holography with MATLAB* (Springer, 2007).
15. T. Latychevskaia and H.-W. Fink, "Inverted Gabor holography principle for tailoring arbitrary shaped three-dimensional beams," *Sci. Rep.* **6**, 26312 (2016).
16. D. P. Kelly, B. M. Hennelly, N. Pandey, T. J. Naughton, and W. T. Rhodes, "Resolution limits in practical digital holographic systems," *Opt. Eng.* **48**(9), 95801 (2009).
17. A. W. Lohmann and D. P. Paris, "Binary Fraunhofer holograms, generated by computer," *Appl. Opt.* **6**(10), 1739-1748 (1967).
18. T. Shimobaba and T. Ito, *Computer holography: Acceleration algorithms and hardware* (CRC Press, 2019).
19. B. G. Chae, "Viewing angle of reconstructed image from digital hologram with enhanced numerical aperture," *arXiv:2004.12543* (2020).